Quantum Electronics **47** (9) 835–841 (2017)

https://doi.org/10.1070/QEL16374

Amplitude/phase modulation and spectrum of the vertical-cavity surface-emitting laser output

M.I. Vas'kovskaya, V.V. Vasil'ev, S.A. Zibrov, V.L. Velichansky, I.V. Akimova, A.P. Bogatov, A.E. Drakin

Abstract. **A new approach has been proposed for analysing the dynamics of the laser field amplitude on the basis of Maxwell's equations. This approach has been used to develop a theory for calculating modulation characteristics of vertical-cavity surface-emitting lasers in the small modulation limit. The present analysis allows one to sequentially examine the dynamics of the amplitude and phase of the electromagnetic field of light in the framework of a single physical model, proceeding from fundamental principles. The proposed approach offers a natural and unique procedure for finding all laser cavity parameters necessary for calculation. An analytical calculation in the 'small'-signal approximation has ensured good agreement with experimental data.**

Keywords: *vertical-cavity surface-emitting laser, modulation characteristics, emission spectrum.*

1. Introduction

Tunable single-frequency diode lasers are widely used in spectroscopy. The principal controlled parameter of laser emission in such applications is its optical frequency (wavelength). The laser emission spectrum is typically controlled by varying the optical length of the laser cavity and, accordingly, its resonance frequency. A new spectroscopic application of diode lasers, based on the coherent population trapping (CPT) effect, has recently emerged and is making rapid progress. One example is the development of frequency standards based on this effect in alkali metal atoms [1, 2]. Such applications impose other requirements for the spectral characteristics of laser emission: one needs at least bichromatic light with a strictly controlled spectral separation (in the gigahertz range) between its optical frequencies.

M.I. Vas'kovskaya, V.V. Vasil'ev, S.A. Zibrov P.N. Lebedev Physical Institute, Russian Academy of Sciences, Leninsky prosp. 53, 119991 Moscow, Russia; Advanced Energy Technologies Ltd., Cheremushkinskii proezd 5, 117036 Moscow, Russia;
V.L. Velichansky P.N. Lebedev Physical Institute, Russian Academy of Sciences, Leninsky prosp. 53, 119991 Moscow, Russia; National Nuclear Research University MEPhI (Moscow Engineering Physics Institute), Kashirskoe sh. 31, 115409 Moscow, Russia; Advanced Energy Technologies Ltd., Cheremushkinskii proezd 5, 117036 Moscow, Russia; e-mail: vlvlab@yandex.ru;
I.V. Akimova, A.P. Bogatov, A.E. Drakin P.N. Lebedev Physical Institute, Russian Academy of Sciences, Leninsky prosp. 53, 119991 Moscow, Russia; e-mail: drakin@sci.lebedev.ru

Received 23 March 2017
Kvantovaya Elektronika **47** (9) 835–841 (2017)
Translated by O.M. Tsarev

One of the sources best suited for this purpose is a vertical-cavity surface-emitting laser (VCSEL) [3] with a pump current modulated at a microwave frequency required for CPT. As a result of pump current modulation, the initially single-frequency diode laser output becomes multifrequency: in addition to the main optical frequency, so-called side frequencies (sidebands) emerge on both the 'blue' and 'red' sides of the spectrum, which are separated from the carrier by a multiple of the modulation frequency. An advantageous feature of VCSELs in the applications in question is their dynamic single-frequency operation. Because of the small dimensions of their cavity, the spectral separation between its eigenfrequencies typically lies in the terahertz range, and losses at such frequencies considerably exceed those for the fundamental oscillation mode. By virtue of the above, such a laser operates on only one spatial (in terms of all three indices) oscillation mode over the entire operating range of pump currents and microwave modulation. For this reason, both the centre frequency and the modulation-induced side components have the same spatial configuration.

The CPT effect and its many applications have been considered in detail in a number of reviews [2, 4, 5]. For use in atomic frequency standards, the two components of light resonant with atomic transitions should meet the following requirements: First, the field amplitudes of the components should be as close as possible to each other (symmetry of the spectrum) and their phase fluctuations should be correlated. Second, the frequency difference between the components should be equal to the frequency of the metrological 0–0 transition in the hyperfine structure with allowance for its shifts (due to variations in the buffer gas pressure and temperature) from the ground state of caesium or rubidium atoms. Modulating the pump current of a VCSEL at half the metrological transition frequency allows these requirements to be satisfied in the simplest way. However, a real spectrum contains, in addition to the first resonance sidebands, the carrier frequency and higher order sidebands. To ensure that optical shifts (changes in the frequency of the metrological transition because of the disturbing effect of optical fields) are small, the intensity of the carrier component should be minimised [6]. It was initially unclear to what extent these requirements could be satisfied by selecting the operation mode of a VCSEL.

Given the above, the objectives of this investigation in the first stage were to assess the feasibility of modelling the emission spectrum of a laser for CPT applications at a small modulation signal and experimentally verify modelling results.

2. Calculation of the amplitudes of spectral components of modulated light from a laser operating on a single spatial mode

Figure 1 shows a schematic diagram of the laser under consideration [3]. Its configuration includes many single-crystal semiconductor layers grown on a substrate, which jointly act as Bragg reflectors of the cavity. In between these layers there is one or a few active layers, which are responsible for gain. The output light leaves the device through a part of the laser surface, S_{out}, as shown in Fig. 1.

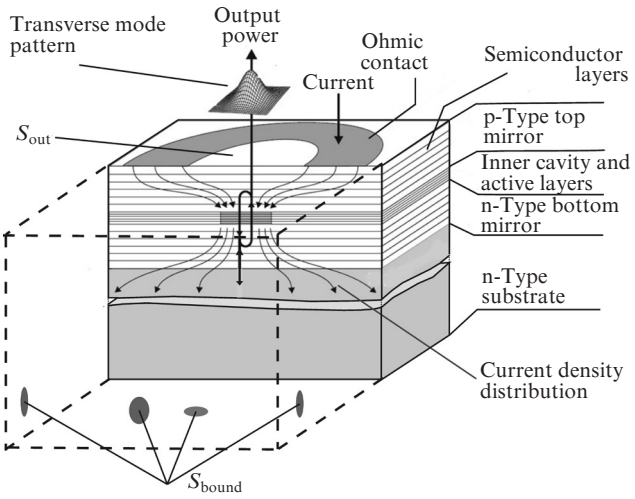

Figure 1. Schematic structure of a VCSEL [3]. The output light leaves the device through a part of the top surface, S_{out}. On the rest of this surface and on the S_{bound} surfaces, the optical field is negligible.

Consider first a physical model of the laser. From the optical point of view, its design is completely determined by the spatial distribution function of the complex dielectric permittivity in some volume V, bounded on one side by the surface S_{out} and on the other sides by the surface S_{bound}, where the optical field is so weak that it can be neglected. In the case of microwave modulation of laser light, the dielectric permittivity ε at the light wave's frequency ω can be represented in the form

$$\varepsilon(r,\omega,N(r,t)) = \varepsilon_0(r,\omega_0,N_s(r)) + \frac{\partial\varepsilon}{\partial\omega}\Big|_{\omega=\omega_0}\Delta\omega + \frac{\partial\varepsilon}{\partial N}\Big|_{N=N_s(r)}\Delta N(r,t),$$
$$\frac{\partial\varepsilon}{\partial N}\Big|_{N=N_s} = -\frac{\sigma(\omega_0)n}{k_0}(R+\mathrm{i}). \quad (1)$$

Here, ω_0 and ε_0 are the laser frequency and dielectric permittivity in a steady state (no pump current modulation: $J(t) = J_0 = \text{const}$); $k_0 = \omega_0/c$; c is the speed of light; $\Delta\omega = \omega - \omega_0$; $N(r,t)$ is the injected electron concentration in the case of current modulation; $N_s(r)$ is the steady-state injected electron concentration that ensures the gain necessary for lasing (threshold concentration); $\Delta N(r,t) = N(r,t) - N_s(r)$; $\sigma(\omega_0)$ is the stimulated transition cross section (differential gain); n is the refractive index of the active layer; and R is the dimensionless amplitude–phase coupling factor.

The injected electron concentration $N(r,t)$ will be treated in factored form, $N(r,t) = N(t)f(r)$, where the dimensionless spatial electron distribution function $f(r)$ is normalised to unity in the origin, i.e. $f(0,0,0) = 1$. In addition, its shape is taken to persist over the entire operating range of pump currents and corresponding output powers. This approximation is justified by the fact that the dimensions of the active region in the lasers under consideration are typically much less or no greater than the electron diffusion length. Then $\Delta N(r,t) = (N(t) - N_{th})f(r)$, where N_{th} is the threshold concentration of injected electrons in the centre of the active region.

Using the important fact that, throughout the operating range of laser output powers, the spatial configuration of the light-wave field amplitude $\mathcal{E}(r,t)$ remains unchanged, the complex part of the amplitude can also be represented in factored form. In a steady state at a constant pump current J_0 well above the threshold current J_{th}, the field amplitude can be represented as

$$\mathcal{E}_0(r,t) = \frac{1}{2}[E_0 e^{-\mathrm{i}\omega_0 t}\boldsymbol{u}(r) + \text{c.c.}]. \quad (2)$$

The complex vector function $\boldsymbol{u}(r)$ characterises the spatial distribution of the amplitude over volume V. For definiteness, without loss of generality we normalise $\boldsymbol{u}(r)$ so that its magnitude in the centre of the active region, with the coordinates $r = (0,0,0)$, is unity, i.e. $|\boldsymbol{u}(0,0,0)|^2 = 1$. Hereafter, $\boldsymbol{u}(r)$ is taken to be known as a solution to an independent problem defined by Maxwell's equations for the steady-state monochromatic field (2) subject to appropriate boundary conditions:

$$E_0 e^{-\mathrm{i}\omega_0 t}\,\mathrm{curl}\,\mathrm{curl}\boldsymbol{u}(r) = k_0^2\varepsilon_0(r,N_s(r),\omega_0)E_0 e^{-\mathrm{i}\omega_0 t}\boldsymbol{u}(r). \quad (3)$$

Pump current modulation, $J(t)$, by a variable component at frequency Ω will lead to electron concentration modulation, $N(t)$, and hence to modulation of the laser output amplitude and phase. In our case, the optical field amplitude $\mathcal{E}(r,t)$, pump current $J(t)$ and electron concentration $N(t)$ can be represented as

$$\mathcal{E}(r,t) = \frac{1}{2}\{[E_0 e^{-\mathrm{i}\omega_0 t} + E_1 e^{-\mathrm{i}\omega_1 t} + E_{-1}e^{-\mathrm{i}\omega_{-1}t}]\boldsymbol{u}(r) + \text{c.c.}\}, \quad (4)$$

$$J(t) = J_0 + J_{th}m(e^{-\mathrm{i}\Omega t} + \text{c.c.}),$$
$$N(t) = N_{th} + (\delta N e^{-\mathrm{i}\Omega t} + \text{c.c.}), \quad (5)$$

where $\omega_{\pm1} = \omega_0 \pm \Omega$; $m = \delta J/(2J_{th})$ is a dimensionless parameter; and δJ and δN are the microwave modulation amplitudes for the current and electron concentration. The small-signal approximation in our model means that the inequality

$$|E_{\pm1}| \ll |E_0|; \quad |\delta N| \ll N_{th}, \quad m \leqslant J_0/(2J_{th}) \quad (6)$$

is fulfilled and that, in analysis, second- and higher order terms can be neglected relative to those in (6). The model formulated above allows $E_{\pm1}$ to be found in analytical form.

It is worth noting that it is not quite correct that the field generated by the sources described by the term $c^{-1}(\partial D/\partial t)$ in Maxwell's equation is represented in the form (4). If a complete representation of the field is needed, in our case Eqn (4)

should be supplemented by fields having a different coordination dependence, e.g. by fields of other transverse modes orthogonal to field (4), scattered-light fields and local fields. It can be shown, however, that, in the case of the integration procedure described below, the contribution of such fields is too small to influence the result. Given this, the representation of the resultant field in the form (4) is acceptable.

Next, substituting the expression for the amplitude of the modulated field (4) into Maxwell's equation we obtain an equation analogous to (3) but with $\varepsilon(r,\omega,N)$ in the form (1) for each frequency under consideration. To separate the $E_{\pm1}$ amplitudes from the total field, we utilise the orthogonality conditions for cavity eigenmodes [7]. To this end, we multiply both sides of this equation by $\boldsymbol{u}(r)$, integrate over the entire volume V and separate terms with identical frequencies, $\omega_{\pm1} = \omega_0 \pm \Omega$. Taking into account (3), we obtain two equations for the E_1 and E_{-1} amplitudes:

$$E_1\int_V \boldsymbol{u}^2(r)\{k_1^2\tilde{\varepsilon}(r,\omega_1) - k_0^2\varepsilon_0(r,\omega_0,N_s(r))\}\mathrm{d}V + E_0k_1^2\frac{\partial\varepsilon}{\partial N}\delta N\int_V \boldsymbol{u}^2(r)f(r)\mathrm{d}V = 0, \tag{7}$$

$$E_{-1}\int_V \boldsymbol{u}^2(r)\{k_{-1}^2\tilde{\varepsilon}(r,\omega_{-1}) - k_0^2\varepsilon_0(r,\omega_0,N_s(r))\}\mathrm{d}V + E_0k_{-1}^2\frac{\partial\varepsilon}{\partial N}\delta N^*\int_V \boldsymbol{u}^2(r)f(r)\mathrm{d}V = 0, \tag{8}$$

$$\tilde{\varepsilon}(r,\omega_{\pm1}) = \varepsilon_0(r,\omega_0,N_s(r)) \pm \Omega\frac{\partial\varepsilon}{\partial\omega}\Big|_{\omega=\omega_0},\quad k_{\pm1} = \frac{\omega_0\pm\Omega}{c}.$$

Omitting the terms proportional to Ω^2 and $\Omega\delta N$ in (7) and (8) and normalising to

$$V_0 = \int_V \varepsilon_0(r,\omega_0,N_s(r))\boldsymbol{u}^2(r)\mathrm{d}V,$$

we obtain the following equations for E_1 and E_{-1}:

$$E_1\frac{2k_0\Omega}{c}(1+\xi) + E_0k_0^2\Gamma\frac{\partial\varepsilon}{\partial N}\delta N = 0, \tag{9}$$

$$E_{-1}\frac{-2k_0\Omega}{c}(1+\xi) + E_0k_0^2\Gamma\frac{\partial\varepsilon}{\partial N}\delta N^* = 0, \tag{10}$$

where we introduced the dimensionless coefficients

$$\xi = \frac{\omega_0}{2V_0}\int_V \boldsymbol{u}^2(r)\,\frac{\partial\varepsilon}{\partial\omega}\Big|_{\omega=\omega_0}\mathrm{d}V,$$

$$\Gamma = \frac{1}{V_0}\int_V \boldsymbol{u}^2(r)f(r)\mathrm{d}V. \tag{11}$$

Here, ξ characterises the dispersion contribution to the energy and its dissipation in the cavity and Γ characterises the fraction of the active region volume in the total cavity volume and is an analogue of the optical confinement factor, which is used in calculations, e.g., for edge-emitting laser diodes.

To solve Eqns (9) and (10), it remains only to find δN. This can be done using the balance equation for the electron concentration in the centre of the active region. The power transferred from an active medium of unit volume to an electromagnetic field is $\omega|\mathcal{E}(r,t)|^2\varepsilon''/(4\pi)$, and the energy per electron is $\hbar\omega$. Therefore, it can be written for the centre of the active region

$$\frac{\mathrm{d}N(t)}{\mathrm{d}t} + \frac{N(t)}{\tau} + \frac{(N(t)-N_{tr})\sigma cn}{8\pi\hbar\omega}|E_0\exp(-\mathrm{i}\omega_0t) + E_1\exp(-\mathrm{i}\omega_1t) + E_{-1}\exp(-\mathrm{i}\omega_{-1}t)|^2 - \frac{J(t)}{eV_{act}} = 0, \tag{12}$$

$$V_{act} = \int_V f(r)\mathrm{d}V,$$

where τ is the spontaneous excited-state lifetime of an electron; N_{tr} is the transparency concentration; and V_{act} is the effective volume of the active region. Substituting expressions (5) for $N(t)$ and $J(t)$ into (12) and separating steady-state terms from terms oscillating at frequency Ω, we obtain for the steady-state part

$$\frac{N_{th}}{\tau} + \frac{\sigma(N_{th}-N_{tr})cn}{8\pi\hbar\omega}|E_0|^2 - \frac{J_0}{eV_{act}} = 0. \tag{13}$$

Given that, at the lasing threshold J_{th}, the laser field amplitude is zero, it follows from (13) that

$$\frac{\sigma(N_{th}-N_{tr})cn}{8\pi\hbar\omega}|E_0|^2 = \eta\frac{N_{th}}{\tau}, \tag{14}$$

where $\eta = (J_0 - J_{th})/J_{th}$ is the relative difference between the pump current and the lasing threshold J_{th}. For the oscillating concentration δN, we obtain from (12), taking into account (14),

$$\delta N = N_{th}\left\{m - \eta\frac{E_0^*E_1 + E_0E_{-1}^*}{|E_0|^2}\right\}(1+\eta\theta-\mathrm{i}\Omega\tau)^{-1},$$
$$\theta = \frac{N_{th}}{N_{th}-N_{tr}}. \tag{15}$$

Equations (9), (10) and (15) constitute a complete system for finding δN and $E_{\pm1}$. To this end, it is convenient to change from $E_{\pm1}$ to dimensionless $v_{\pm1}$ defined by $E_{\pm1} = v_{\pm1}E_0$ and use not Eqn (10) but its complex conjugate. Substituting δN from (15) into (9) and (10), we obtain a system of two linear equations in $v_{\pm1}$:

$$v_1 - (\tilde{R}+\mathrm{i})a(\Omega)[m - \eta(v_1 + v_{-1}^*)] = 0,$$
$$v_{-1}^* + (\tilde{R}-\mathrm{i})a(\Omega)[m - \eta(v_1 + v_{-1}^*)] = 0. \tag{16}$$

Here we use the following designations:

$$\tilde{R} = \mathrm{Re}[\Gamma(R+\mathrm{i})/(1+\xi)]/\tilde{\Gamma},$$
$$\tilde{\Gamma} = \mathrm{Im}[\Gamma(R+i)/(1+\xi)], \tag{17}$$

$$a(\Omega) = \frac{\Omega_0}{2\Omega(1+\eta\theta - \mathrm{i}\Omega\tau)},\ \Omega_0 = \tilde{I}\sigma N_0 cn. \tag{18}$$

The solution to system (16) has the form

$$v_1 = \frac{m(\tilde{R}+\mathrm{i})}{2}\frac{\Omega_0}{\Omega(1+\eta\theta)+\mathrm{i}(\eta\Omega_0-\Omega^2\tau)},$$
$$v_{-1} = v_1^*\frac{\tilde{R}+\mathrm{i}}{\mathrm{i}-\tilde{R}}. \tag{19}$$

The light intensity at the frequencies $\omega_{\pm1} = \omega_0 \pm \Omega$ is then $I_{\pm1} = I_0|v_1|^2$.

The presence of three spectral components at frequencies ω_0 and $\omega_{\pm1}$ can be thought of as amplitude/phase modulation of the light at the centre frequency ω_0. For example, if the total output power $\mathcal{P}(t)$ is written as $\mathcal{P}(t) \approx \mathcal{P}_0 + \delta\mathcal{P}\sin(\Omega t + \phi)$, we obtain for the amplitude modulation of the total output beam power, $\delta\mathcal{P}$, and its phase shift, ϕ, relative to the modulation current:

$$\delta\mathcal{P} \approx 2m\mathcal{P}_0\left|\frac{\Omega_0}{\Omega(1+\eta\theta)+\mathrm{i}(\eta\Omega_0-\Omega^2\tau)}\right|,$$
$$\tan\phi \approx \frac{\eta\Omega_0-\Omega^2\tau}{\Omega(1+\eta\theta)}, \tag{20}$$

where $\mathcal{P}_0$ is the steady-state output power (without modulation). To represent phase modulation, we replace relation (4) for the time-dependent field amplitude by the approximate relation

$$E_0\exp(-\mathrm{i}\omega_0 t) + E_1\exp(-\mathrm{i}\omega_1 t) + E_{-1}\exp(-\mathrm{i}\omega_{-1}t)$$
$$\approx E_0 e^{-\mathrm{i}\omega_0 t - \mathrm{i}\varphi(t)},$$
$$\varphi(t) \approx \frac{mR\Omega_0}{\left|\Omega(1+\eta\theta)+\mathrm{i}(\eta\Omega_0-\Omega^2\tau)\right|}\sin(\Omega t+\phi). \tag{21}$$

Even though relations (20) and (21) are only approximate, the associated error falls within the small modulation amplitude approximation used in our physical model.

Thus, relations (19)–(21) completely determine all the spectral and dynamic characteristics of the laser output in the case of the small-signal modulation of the pump current. The parameters of the cavity and its active region in (19)–(21) can be found as solutions to a separate problem, if additional information regarding the laser design is available.

3. Experimental

We studied ULM Photonics VCSELs (Philips) with the following characteristics: wavelength $\lambda = 795$ nm, threshold current $J_{th} = 0.58$ mA, output power $P_{opt} \leqslant 1$ mW and slope efficiency $\varkappa = 0.3$ W A^{-1}. Figure 2 shows a schematic of the experimental setup.

The constant pump current and microwave modulation current are fed to the laser through a decoupler, which prevents the low-frequency and microwave oscillators from influencing each other. The constant pump current level and the sawtooth current modulation amplitude are controlled by the power supply unit of the laser (the microwave power values indicated below refer to the oscillator output power, which may differ from the power directly delivered to the active region of the laser because of the imperfect matching). The laser light passes through an optical isolator and half-wave plate and is split by a polarising cube into two optical channels. Combining the half-wave plate and polarising cube allows the total optical power to be redistributed between the channels. In one channel, the light passes through an ^{87}Rb vapour cell and is detected by a photodetector. In the other channel, the emission spectrum is analysed using a Fabry–Perot interferometer with a free spectral range of 24 GHz. The signals from both photodetectors are fed to an oscilloscope.

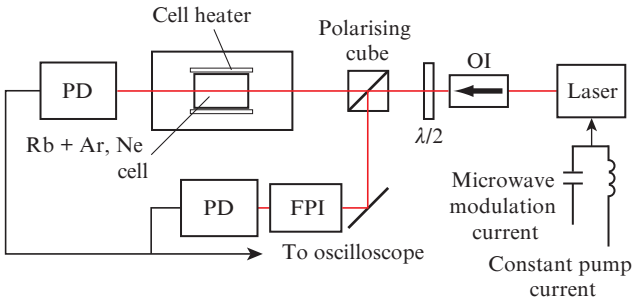

Figure 2. Schematic of the experimental setup: (FPI) Fabry–Perot interferometer; (PD) photodetector; (OI) optical isolator.

Thus, the system allows us to simultaneously measure the light power–current (L–I) characteristic and tune the laser frequency to the Rb D_1 line (from the presence of absorption lines in the L–I curve) in the former channel and monitor the emission spectrum in the latter channel. This is demonstrated in Fig. 3, which shows the L–I curve and the transmission signal of the Fabry–Perot interferometer in the absence of microwave current modulation.

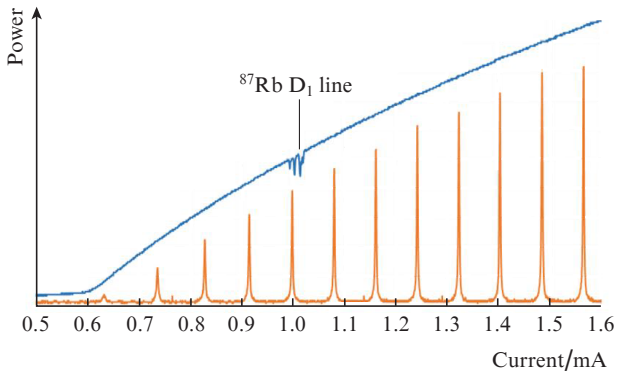

Figure 3. Power–current curve of the ULM laser measured with the photodiode located behind the Rb vapour cell (upper curve) and transmission resonances of a Fabry–Perot interferometer with a free spectral range of ~24 GHz (lower curve).

An increase in pump current is accompanied by an increase in the temperature of the optical medium in the laser cavity and, as a consequence, by an increase in its refractive index. This leads to a monotonic decrease in laser frequency with increasing pump current. As a result, the interferometer

output signal (the latter channel) has the form of periodic transmission peaks, each corresponding to the laser frequency sequentially passing through a successive transmission resonance of the interferometer. The spacing between neighbouring peaks corresponds to the temperature-induced change in laser frequency by the free spectral range of the interferometer (24 GHz).

The absence of side resonances in the transmission of the interferometer confirms that the light is single-mode. A polychromatic spectrum of the laser can be obtained by either scanning the interferometer or linearly varying the pump current, thereby shifting the laser spectrum as a whole. In Fig. 4, the latter possibility is illustrated by a typical laser spectrum obtained by sweeping the constant pump current containing a microwave modulation component of constant amplitude. With such a measurement procedure, one oscilloscope trace shows a family of spectra, each corresponding to its own 'constant' pump current and the same microwave modulation amplitude, with the laser spectrum sequentially measured using different (immobile) interferometer resonances. The steep slope of the laser frequency–current tuning curve causes no significant error, because the laser output power varies little in response to the small variation in the current that enables the laser spectrum to be measured. The oscilloscope trace in Fig. 4 demonstrates the entire evolution of the laser spectrum in the modulation regime in response to changes in constant pump current at a given microwave field power level.

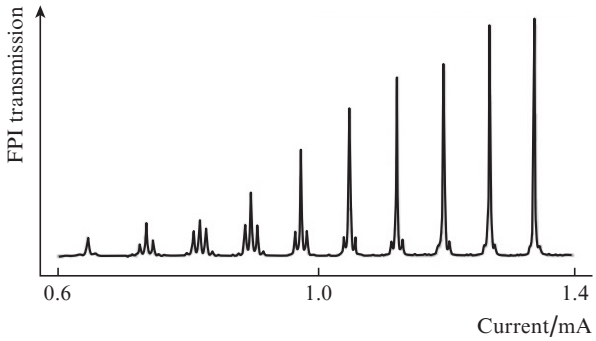

Figure 4. Evolution of the ULM laser emission spectrum in response to changes in the constant component of a microwave-modulated current. The microwave modulation power is –3 dBm.

Figure 5 presents experimental data illustrating the effect of constant pump current on the ratio of the sideband power $P_{\pm1}$ to the power P_0 at the carrier frequency for three modulation frequencies: $\Omega/2\pi = 2.0$, 3.4 and 4.0 GHz (the data were obtained in the same way as those in Fig. 4). The solid line represents calculated $|v_1|^2$ as a function of the constant pump current component for a laser with the following parameters: $\tau = 1$ ns, $\Omega_0 \approx 490$ rad s^{-1} and $\theta \approx 10.1$ (note that the 'transparency' current calculated for $\theta = 10.1$ is $J_{tr} = 0.52$ mA). All the curves are normalised to the maximum. There is good agreement between the experimental data and calculation results. It is worth noting that, even though there are three adjustable parameters, concurrent agreement between the calculation results and experimental data at all three different frequencies is ensured by only one of their combinations. This

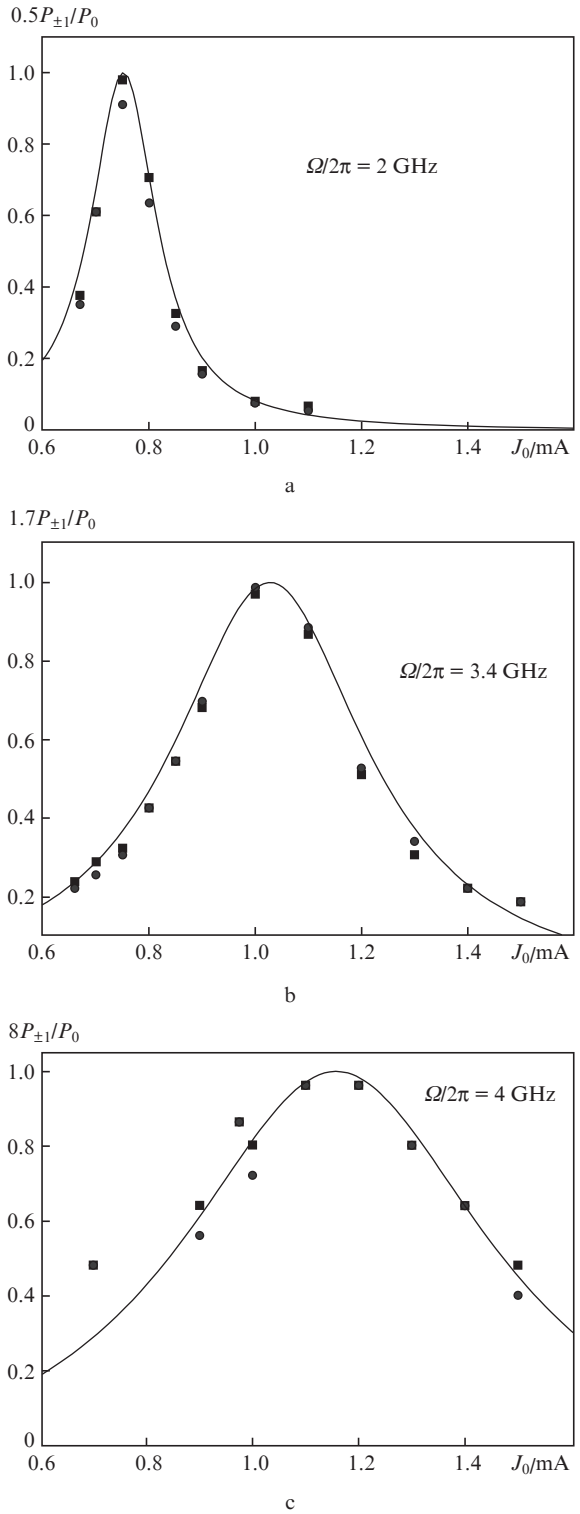

Figure 5. Measured and calculated $P_{\pm1}/P_0$ power ratios as functions of pump current at three microwave modulation frequencies: (■) P_{-1}, (●) P_{+1}. The parameters used in the calculation are $\tau = 1$ ns, $J_{th} = 0.58$ mA, $\Omega_0 \approx 490$ rad s^{-1} and $\theta \approx 10.1$.

is additional evidence that the proposed theory and the calculations based on it are sufficiently adequate.

Indeed, from the relation $|v_1|^2 = I_{\pm1}/I_0$ we readily obtain an expression for the pump current (parameter η) corresponding to the maximum in $|v_1|^2$:

$$\eta_{\max} = \frac{\tau\Omega_0 - \theta}{\theta^2 + (\Omega_0/\Omega)^2},$$

or

$$\frac{1}{\Omega^2} = \frac{1}{\eta_{\max}}\left(\frac{\tau - \theta/\Omega_0}{\Omega_0}\right) - \left(\frac{\theta}{\Omega_0}\right)^2. \quad (22)$$

It follows from this expression that there is a linear relation between Ω^{-2} and $\eta_{\max}^{-1}$, i.e. these quantities should lie on a single straight line with a slope $(\tau - \theta/\Omega_0)/\Omega_0$ and a vertical intercept θ^2/Ω_0^2. The experimental data are rather well represented by this straight line. In such a way, we can obtain a relation between the parameters Ω_0, θ and τ for a given sample, which would allow us to express e.g. the parameters Ω_0 and θ trough τ. The lifetime τ, determined by spontaneous recombination, is a material parameter of the medium in the active region. Its typical value for 'direct' transitions is $\sim$1 ns, which also ensures the best agreement between the calculation results and experimental data in Fig. 5.

The above results were obtained at a small current modulation, limited by -8 dBm. Under such conditions, the optical spectrum contains a strong line at the carrier frequency and one, 'weak' sideband on each side of the 'strong' line. By contrast, in the case of applications utilising CPT it is desirable to have a 'weak' line at the carrier frequency and two 'strong' sidebands of equal intensities. One way, obvious at first sight, to achieve this is to increase the amplitude of the microwave modulation of the pump current.

Figure 6 shows a typical laser emission spectrum obtained in such a case. It can be seen that the result is not quite what was expected. First, there is an increased number of spectral components on account of the formation of extra lines separated by $\pm 2\omega_0$, $\pm 3\omega_0$ etc. from the carrier frequency ω_0. Qualitatively, this is clear: the number of harmonics increases with modulation amplitude. Second, the spectrum may be not symmetric with respect to the frequency ω_0. These features in the behaviour of the laser may lead to an additional, poorly controlled frequency shift of the CPT resonance and, hence, to an additional limitation on its ultimate capabilities in metrology.

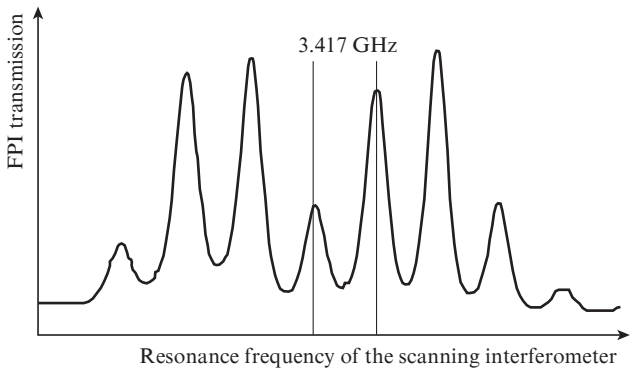

Figure 6. Characteristic laser emission spectrum in the case of strong modulation. Operating current $J = 1$ mA; microwave modulation power $P = 1.6$ mW. The spectral linewidth $\Delta\nu \approx 1.5$ GHz is mainly determined by the interferometer resolution ($\Delta\nu_{\mathrm{FPI}} \approx 1.4$ GHz).

Clearly, the above features in the behaviour of the laser cannot be analysed in the framework of the present calculations, because the physical situation ('strong' modulation) is beyond the approximation used in the calculations.

4. Discussion and conclusions

A new approach has been proposed for analysing the dynamics of the laser field amplitude on the basis of Maxwell's equations. This approach has been used to develop a theory for calculating modulation characteristics of VCSELs.

In contrast to a widely used analysis of the dynamics of diode lasers on the basis of so-called rate equations (see e.g. Refs [3, 8]), which employ the field amplitude rather than the field intensity, the present analysis allows one to sequentially examine the dynamics of the amplitude and phase of the electromagnetic field of light in the framework of a single physical model. Note that rate equations do not contain the field phase as a variable, because it 'disappears' in going to intensity. Basically, rate equations describe the dynamics of the energy ('photon density') in the cavity and reflect no more than the law of conservation of energy. They miss the properties of the electromagnetic field in the cavity, which appear in Maxwell's equations. For this reason, analysis in terms of rate equations requires a phenomenological introduction of e.g. parameters such as the photon lifetime or the field phase and its dynamics through the variation in the optical frequency of the cavity in response to inversion changes. In the case of a VCSEL, this operation is far from being obvious. The proposed approach offers a natural and unique procedure for finding all cavity parameters necessary for calculation. Clearly, the wave equation was used previously as well to investigate the dynamics of laser operation (see e.g. Ref. [9]), but the small number of such studies and the limited applicability of the physical models involved make it impossible to use their results for our purposes.

The present analytical calculation in the 'small'-signal approximation ensured good agreement with experimental data, strongly suggesting that the proposed theory can be used to model spectral characteristics of VCSELs in order to optimise their performance in metrological applications of CPT resonance. Note that the phases of the sideband fields are 'tightly' locked to each other by the common modulation signal and the single field amplitude at the centre frequency, which corresponds to the most favourable situation for CPT resonance.

Because of the approximations used here, the present calculations fail to give comprehensive answers to all questions that arise in analysis of experimental data obtained under various laser operation conditions, including those best suited to application in CPT clocks. Under such conditions, a significant part of the optical power in the spectrum is accounted for by higher order sidebands (Fig. 6). In such a case, the increase in CPT resonance frequency caused by the light shift due to the carrier and first sidebands may be compensated for by the opposite shift due to higher order sidebands [6].

Nevertheless, we are led to conclude that, in the case of numerical calculation, there are no fundamental obstacles to sequentially abandoning the 'small'-signal approximation or the simplified complex dielectric permittivity function, which can be replaced by a function that takes into account the possible spectral mismatch between the cavity mirrors and 'material' gain. This will allow one to make the model of the laser

more realistic and will extend the applicability area of results obtained by calculations in the framework of the model.

References

1. Knappe S., Shah V., Schwindt P.D., Hollberg L., Kitching J., Liew L.A., Moreland J. *Appl. Phys. Lett.*, **85**, 1460 (2004).
2. Knappe S. *Compr. Microsyst.*, **3**, 571 (2007).
3. Michalzik R., in *VCSELs: Fundamentals, Technology and Applications of VCSELs* (Berlin–Heidelberg: Springer-Verlag, 2013) p. 19.
4. Agap'ev B.D., Gornyi M.B., Matisov B.G., Rozhdestvenskii Yu.V. *Phys. Usp.*, **36** (9), 763 (1993) [*Usp. Fiz. Nauk*, **163** (9), 1 (1993)].
5. Arimondo E., in *Progress in Optics XXXV* (Amsterdam: Elsevier, 1996) p. 259.
6. Zhu M., Cutler L.S., in *32nd Annual Precise Time and Time Interval (PTTI) Meeting* (Reston, VA, 2001) p. 311.
7. Vainshtein L.A. *Elektromagnitnye volny* (*Electromagnetic Waves*) (Moscow: Radio i Svyaz', 1988) p. 354.
8. Olshansky R., Hill P., Lanzisera V., Powazinik W. *IEEE J. Quantum Electron.*, **QE-23**, 1410 (1987).
9. Piazzolla S., Spano P., Tamburrini M. *IEEE J. Quantum Electron.*, **QE-22**, 2119 (1986).